AIP | Applied Physics Letters

Detection of extended interstitial chains in iondamaged silicon

T. Y. Tan, H. Föll, and W. Krakow

Citation: Applied Physics Letters **37**, 1102 (1980); doi: 10.1063/1.91888
View online: http://dx.doi.org/10.1063/1.91888
View Table of Contents: http://scitation.aip.org/content/aip/journal/apl/37/12?ver=pdfcov
Published by the AIP Publishing

Detection of extended interstitial chains in ion-damaged silicon

T. Y. Tan, H. Föll, and W. Krakow
IBM Thomas J. Watson Research Center, Yorktown Heights, New York 10598

(Received 25 August 1980;accepted for publication 13 October 1980)

We have carried out a high-resolution electron microscope lattice imaging study of As^+ ion-damaged silicon. Along with dislocation dipoles and intermediate defect configurations from which the dislocation dipoles are generated, ⟨110⟩ chain-type defects have also been detected. By image matching of the experimental and calculated micrographs, it is established that about 100% more interstitial silicon atoms were incorporated in the defective chain. A structure model of this defect is proposed wherein a di-interstitial occupying the ⟨100⟩ split position is incorporated into every available site along a ⟨110⟩ chain.

PACS numbers: 61.70.Bv, 61.70.Jc, 61.80.Jh

For the past twenty-five years defect creation in semiconductors due to radiation damage has been extensively studied. From electron paramagnetic resonance (EPR) experiments, the configuration of a number of vacancy-related defects in silicon has been well established.[1] These include the charge single vacancy,[2] di-vacancy,[3] four-vacancy cluster,[4] and a number of vacancy-impurity atom complexes.[1,5] There is much less experimental information concerning the silicon self-interstitial atoms; however, a di-interstitial configuration was detected by EPR.[6] For the single interstitial atom, it was long held that it would occupy the tetrahedral, the hexagonal, the bond-centered, or the split-⟨100⟩ position in the diamond lattice. The split-⟨100⟩ configuration is thought to have the lowest energy, followed by the bond-centered, the hexagonal, and the tetrahedral configurations, respectively.[1] EPR experiments rely on the detection of the hyperfine (HF) spectrum produced by the dangling or distorted bonds, and they are interpreted by comparision to the calculated electronic states of the defects. If the number of point defects incorporated in a cluster exceeds a few, the HF interactions may produce a band and the spectra become uninterpretable. EPR, therefore, is not particularly suited to investigate the defect formed if the damage is extensive, as in the case of ion implantation. Here, extended defects, primarily in the form of dislocation loops, may be produced. When the size of the dislocation loops exceeds a few hundred Å they may be readily analyzed using transmission electron microscopy (TEM) by observing their strain field behavior by diffraction contrast. For smaller defects, conventional TEM will cease to provide useful information.

There is no easy experimental way to bridge the gap between the observation of point defects by EPR and the TEM investigation of more extended defects. The manner by which point defects condense into extended defects therefore has not been extensively discussed in the literature. To address this subject, we have recently modeled the point-defect condensation process of dislocation nucleation.[7,8] Because of dangling bond considerations necessary for covalent crystals, it was reasoned that dislocations nucleate in the form of narrow dipoles elongated in the ⟨110⟩ direction as opposed to small circular loops in the case of metals. Before dislocation dipoles are generated, the point defects must first condense into some linear, "intermediate defect" configurations (IDC's), a step which has no direct parallel in metals. The intermediate defect configurations consist of non-six-membered atomic rings (when viewed from the ⟨110⟩ direction) for which, at most, only one dangling bond may be present for each point defect incorporated. A high-resolution electron microscope study of As^+ ion-implanted silicon showed this model to be essentially correct in the sense that dislocation dipoles as well as IDC's were observed. This subject will be reported elsewhere.[9]

All IDC's considered so far may be derived from a generalization of already known point-defect chain configurations, e.g., the four-vacancy and the multi-interstitial chains.[1] There are, however, many possible ways of forming point-defect aggregates and those which lead to IDC's are but a limited fraction. In consequence, it is possible that dislocations, loops and dipoles, and IDC's as well as other extended defects are all present simultaneously, especially if the sample temperature is not too high during irradiation. In this letter we report the detection of point-defect chains which consist of silicon di-interstitials. Whereas dislocation dipoles and IDC's, when viewed along ⟨110⟩, are easily identified because of significant configurational changes in the lattice images, the di-interstitial chain has almost no lattice distortion and its detection therefore constitutes a more difficult problem. In this paper we show that the proper use of high-resolution electron microscopy constitutes a suitable

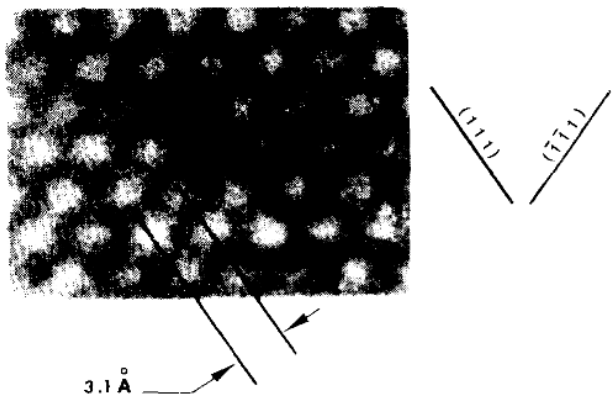

FIG. 1. Experimental image showing the contrast behavior of a defective [1$\bar{1}$0] chain at the center of the micrograph.

 003-6951/80/241102-03$00.50

method of studying defect structures where EPR experiments or conventional TEM may not yield meaningful information.

For our experiments, p-type, 12-Ω cm, $\langle 001 \rangle$ oriented silicon wafers were implanted with As^+ ions at 80 keV to a dose of $8 \times 10^{15}/cm^2$ at 100-μA ion current. This dose of implanation created a layer of amorphous silicon of about 800 Å in thickness. In the crystalline material below the amorphous layer may defects formed *in situ* during the implanation process owing to the high dose rate. $\langle 110 \rangle$ oriented cross-sectional thin foils, about 200 Å thick, were prepared from these wafters and examined in a Siemens 102 electron microscope at 125 kV. Defects were studied by lattice imaging techniques with the foil oriented in $\langle 110 \rangle$ and with seven Bragg beams, 000, $\pm \bar{1}\bar{1}1$, ± 111, and ± 002, included in the objective-lens aperture.

As a result of this imaging study, we have detected the dislocation dipoles and the IDC's,[9] as well as the defect discussed in this letter (see Fig. 1). This micrograph shows a lattice images obtained from the second phase contrast zone in an underfocus setting of the objective lens ($\Delta f \sim 1000$ Å, $Cs = 1.9$ mm and axial illumination) for which the white dots are interpreted as a chain of two unresolved columns of atoms lying 1.36 Å apart. Here it is seen that the white dots exhibit relatively uniform brightness except at the defect center, which shows diminished brightness and size, while its immediate surrounding is a cross-shaped area somewhat darker than the other dark regions. There is no detectable strain or configurational change associated with this white dot, and this contrast behavior can only arise from the fact that the scattering ability of the constituents of the atomic chain related to the white dot are different from the surrounding normal silicon atom chains. Thus, this chain may have incorporated a large number of vacancies or self-interstitials or impurity atoms.

At this stage it is essential to obtain calculated images which can be compared to the experimental image and thus allow to determine whether the defective chain contains vacancies or interstitials. Such images were calculated by using a computer program based on the slice approach of multi-

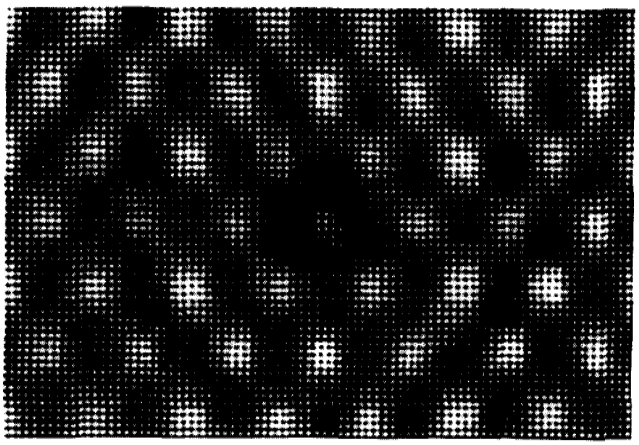

FIG. 2. Calculated image wherein the defective [1$\bar{1}$0] chain was assumed to have incorporated 100% more atoms. The square appearance of the white dots is entirely due to the font size and raster effect of the printer.

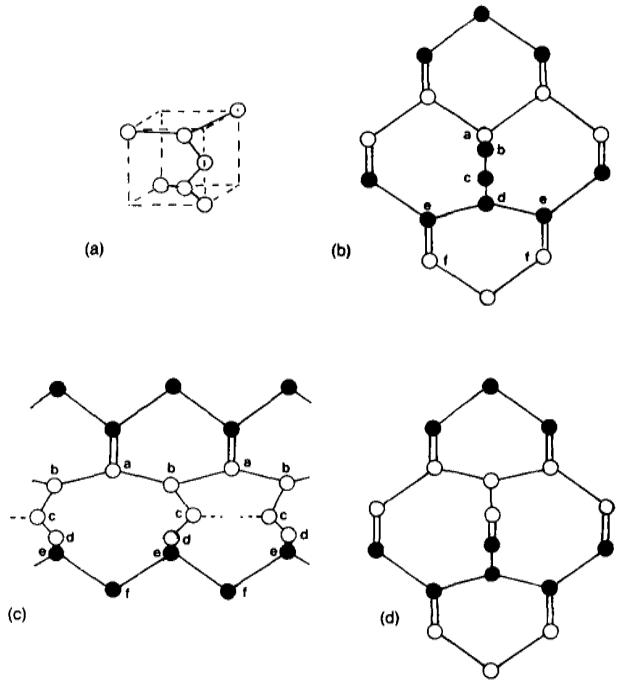

FIG. 3. Atomic models of the defect: (a) The [001] split di-interstitial, oblique view. (b) and (c) the [1$\bar{1}$0] chain of [001] split di-interstitial. (b) is a [1$\bar{1}$0] projection of the chain and matrix, while (c) is a [110] projection which shows some further possible bond reconstructions (dotted line). (d) An alternative way of forming a [1$\bar{1}$0] chain to incorporate 100% more silicon atoms.

beam dynamical theory.[10] This program is capable of calculating diffraction patterns of 256×256 diffraction points in reciprocal space for any given film thickness. Electron micrographs are then obtained by including the appropriate electron-microscope parameters, such as electron wavelength, objective lens spherical abberration, defocus, and beam tilt. For images from 111-type diffraction spots in the second defocus zone, the computed images of the defective chain showed contrast changes for the incorporation of either vacancies or interstitials. For the vacancy case, however, the white dot becomes brighter and the image is, in general, complementary to the experimental image. With the incorporation of 100% more silicon atoms in the chain, the calculated image, Fig. 2, shows an almost exact match with the experimental image (compare Fig. 2 to Fig. 1). The white dot in Fig. 2 is now smaller in size with a somewhat decreased brightness, and its surrounding dark region appears cross shaped and darker than other dark regions in the micrograph. Because of the close match, we conclude that the defective chain in Fig. 1 may be interpreted as having incorporated 100% or near 100% more silicon atoms. If some impurity atoms, e.g., As, instead of silicon self-interstitials, were incorporated, then owing to its larger scattering amplitude, less than 100% of atoms may have been incorporated. The possibility that the observed effect may be due to surface contaminants has been safely ruled out because (i) Similar effects are not found in undamaged samples. And (ii) the contrast anomaly occurred at only one atomic chain site, and our calculations show it will take a large number (half the number of silicon atoms in the chain) of even mercury atoms

stacking up as a pillar on the surface to produce this effect, which is a highly unlikely situation. If the number of interstitials incorporated in the chain are reduced, e.g., to 50%, the same contrast behavior is observed, but the intensity differences are not as pronounced; we have observed several such cases.

Having established the interstitial nature of the defect, we now examine how these interstitials may be incorporated, assuming that they are silicon self-interstitials. In an EPR study of neutron-irradiated silicon, Lee, Gerasimenko, and Corbett[6] proposed a model for the ⟨100⟩ split di-interstitial, in a positive charge state [see Fig. 3(a)]. We now propose that the simplest possible structure of the present defect is an extended [1$\bar{1}$0] chain of these di-interstitials [Figs. 3(b) and 3(c)]. In this chain the number of additional atoms is now 100% of a normal [1$\bar{1}$0] chain of atoms, as required from the foregoing image matching considerations. Lee *et al.*[1,6] further demonstrated that for the single di-interstitial defect, a stable configuration is reached if it is dilated in [001] direction by about 0.22 Å. These small displacements should not be detectable in our present microscope observations, and indeed we have not observed any significant lattice strains. The migration energy of the di-interstitial is estimated to be 0.6 eV,[6] and it is therefore a relatively stable type of defect. An alternative for the di-interstitial chain was also considered; this is shown in Fig. 3(d). In this model, however, the dilations in the [001] direction exceed an interatomic distance.[11] Consequently, the energy is larger and this kind of displacement is not observed in the present experiment.

In the conclusion, image matching of experimental and calculated micrographs has allowed us to identify a [1$\bar{1}$0] chain of silicon atoms containing 100% more silicon atoms than normal chains. The most probable model for this defect is a di-interstitial chain. This defect appears to be stable and does not directly change into an IDC and therefore will not directly evolve into dislocations.

The authors wish to thank Dr. K. N. Tu for encouragement, Dr. Y. H. Lee for helpful discussions, and Professor S. L. Sass for the use of the Cornell Siemens 102 electron microscope.

[1]For a review, see J. W. Corbett and J. C. Bourgoin, in *Point Defects in Solids*, edited by J. H. Crawford and L. M. Slifkin (Plenum, New York 1976), Vol. 2, p. 15.
G. D. Watkins, in *Radiation Damage in Semiconductors* (Academic Press, New York 1965), p. 97.
[3]G. D. Watkins and J. W. Corbett, Phys. Rev. **138**, A543 (1965).
[4]K. L. Brower, Radiat. Eff. **8**, 213 (1971).
[5]G. D. Watkins, J. W. Corbett, and R. M. Walker, J. Appl. Phys. **30**, 1198 (1959).
[6]Y. H. Lee, N. N. Gerasimenko, and J. W. Corbett, Phys. Rev. B **14**, 4506 (1976).
[7]T. Y. Tan and H. Foell, Bull. Am. Phys. Soc. **25**, 372 (1980).
[8]T. Y. Tan, Philos. Mag. (to be published).
[9]T. Y. Tan and H. Foell (unpublished).
[10]W. Krakow (unpublished).
[11]Y. H. Lee (private communications), 1980.

Molecular beam epitaxial GaAs heteroface solar cell grown on Ge

D. L. Miller and J. S. Harris, Jr.
Rockwell International Electronics Research Center, Thousand Oaks, California 91360

(Recieved 28 July 1980; accepted for publication 13 October 1980)

GaAs/AlGaAs heteroface solar cells having AM1 efficiencies up to 17% have been grown by molecular beam epitaxy (MBE) directly on Ge (100) substrates. These cells on Ge have efficiencies identical to cells grown simultaneously on GaAs. The cells reported here are the highest efficiency MBE solar cells reported to date and are the first high-efficiency GaAs solar cells grown directly on Ge by MBE.

PACS numbers: 84.60.Jt, 68.55. + b

High-efficiency GaAs solar cells are promising devices for terrestrial and space electrical power production. Efficiencies as high as 22.9% at AM1, 1 sun,[1] and 24.7% at AM1, 180 suns[2] have been reported. AM0 efficiencies up to 17.2% at 1 sun have also been achieved.[3] Efficiencies about 30% (AM1) are theoretically possible using multiple-bandgap (multicolor) configurations.[4]

The cost of the GaAs single-crystal substrate material used almost exclusively now for the growth of high-efficiency GaAs solar cells has been one of the largest factors contributing to the high cost of these cells. The growth of GaAs on Ge substrates could potentially lower cell costs, as well as provide advantages in light-weight and polycrystal cell applications. These points have been discussed extensively.[5]

We report here the growth of high-efficiency GaAs/AlGaAs heteroface solar cells by molecular beam epitzxy directly on Ge. These cells exhibit electrical and optical characteristics identical to cells grown simultaneously on a GaAs substrate, and exhibit optical conversion efficiencies as high as 17% under simulated AM1 illumination. Efficient solar cells have been grown previously on Ge substrates by vapor phase epitaxy (21% AM1 efficiency), and on GaAs substrates by MBE[7] (16% AM1 efficiency). This is, to our knowledge, the first report of high-efficiency solar cells grown by MBE directly on Ge substrates.

The GaAs solar cell growth was done by MBE in a

 003-6951/80/241104-03$00.50